NASA
TP
1947
c.1

NASA
Technical
Paper
1947

February 1982

TECH LIBRARY KAFB, NM
0067653

Surface Chemistry and Wear Behavior of Single-Crystal Silicon Carbide Sliding Against Iron at Temperatures to 1500° C in Vacuum

Kazuhisa Miyoshi
and Donald H. Buckley

LOAN COPY: RETURN TO
AFWL TECHNICAL LIBRARY
KIRTLAND AFB, N. M.

NASA

TECH LIBRARY KAFB, NM
0067653

NASA Technical Paper 1947

1982

Surface Chemistry and Wear Behavior of Single-Crystal Silicon Carbide Sliding Against Iron at Temperatures to 1500° C in Vacuum

Kazuhisa Miyoshi
and Donald H. Buckley
Lewis Research Center
Cleveland, Ohio

NASA
National Aeronautics
and Space Administration

Scientific and Technical Information Branch

Summary

An investigation was conducted to examine the surface of silicon carbide at various temperatures to 1500° C by X-ray photoelectron and Auger electron spectroscopies. Also examined was the wear and metal transfer behavior of a single-crystal silicon carbide surface in contact with polycrystalline iron. Surface analyses and sliding friction experiments were conducted with the silicon carbide {0001} surface in a vacuum system of 10^{-8} pascal. All friction experiments were conducted with a load of 0.2 newton, at a sliding velocity of 3×10^{-3} meter per minute, and in a vacuum of 10^{-8} pascal (10^{-10} torr).

The results of the investigation indicate that at and below 800° C carbide-carbon and silicon are primarily seen on the silicon carbide surface. Above 800° C graphite increases rapidly with an increase of temperature. The outermost surfacial layer, which consists of mostly graphite and very little silicon at temperatures above 1200° C is about 2 nanometers thick. An apparent thickness of a layer, which consists of a mixture of graphite, carbide, and silicon is about 100 nanometers.

The higher the sliding temperature up to 800° C, the more the metal transfer that is observed to occur to the silicon carbide. Above 800° C there was a transfer of a rough, discontinuous, and thin iron debris instead of the smooth, continuous, and thin iron film that was observed at and below 800° C. Two kinds of fracture pits were observed on the silicon carbide surface: (1) a pit with a spherical particle and (2) multiangular-shaped pit. The former pit may be produced by a mechanism of a spherical-shaped fracture along a circular stress trajectory under the load in the elastic deformation zone. The spherical fracture pits have generally been observed only at sliding temperatures of 400° to 800° C, where the friction is high. The multiangular fracture pit is produced by primary and secondary cracking along the cleavage planes {0001}, {10$\bar{1}$0}, and {11$\bar{2}$0}.

Introduction

In two previous papers we have described the significant temperature influence on the surface chemistry and friction properties of silicon carbide at temperatures to 1500° C (refs. 1 and 2). Above 400° C, in addition to silicon, carbide-carbon and graphite are the primary species on the silicon carbide surface. At 800° C the silicon and carbide-carbon are at a maximum intensity in the XPS spectra. And above 800° C the graphite increases rapidly on the surface with an increase in temperature, while the carbide-carbon and silicon surface concentrations decrease with increasing temperature.

The friction properties of the silicon carbide {0001} surfaces in contact with iron at various sliding temperatures indicated that the coefficients of friction were generally higher at temperatures to 800° C and were 0.6 to 0.9. Above 800° C the coefficient of friction decreases rapidly to a value of about 0.2. The rapid decrease in friction above 800° C correlated with the graphitization of the silicon carbide surface.

We have herein extended the above study to an investigation of the depth profile of the graphite layer on the silicon carbide. A further investigation was conducted to examine the tribological properties of the surface, such as the nature of the wear of the silicon carbide and metal transfer to the silicon carbide. The effects of temperature and the presence of the graphite layer on wear and metal transfer is described.

Sliding friction experiments were conducted with a single-crystal silicon carbide {0001} surface in contact with a polycrystalline iron surface. All friction experiments were conducted with a load of 0.2 newton, at a sliding velocity of 3×10^{-3} meter per minute, at a sliding time of 40 to 60 seconds, and in a vacuum of 10^{-8} pascal (10^{-10} torr) at temperatures to 1200° C. The mean contact pressure according to Hertz is 7.9×10^{8} pascals at room temperature. The region of contact will be bounded by a circle with a radius of about 9 micrometers.

Materials

The single-crystal silicon carbide used in the experiment was a 99.9 percent pure compound of silicon and carbon. The unit cell of α-SiC is hexagonal with a equal to 0.30817 nanometer, c equal to 1.51183 nanometers, and 21 molecules per unit cell (refs. 1 and 2). The method of growth is carbon arc. The {0001} plane was nearly parallel to the sliding surfaces examined herein. X-ray back reflection Laue photographs were taken to establish the exact bulk orientation of the crystals after they had been polished with a diamond powder (3 μm diameter) and then with an aluminum oxide powder (1 μm diameter).

Specimens were within ±2° of the low index {0001} plane. The silicon carbide specimens were in the form of flat platelets and had a mean surface area of about 70 square millimeters. The roughness of the mirror-polished silicon carbide surfaces measured by surface profilometer was 0.1 micrometer for the maximum height of irregularities. The iron was polycrystalline and 99.99 percent pure. The method of preparation is electron-beam zone refining. The radius of the iron pin specimen was 0.79 millimeter.

Apparatus

Two ultrahigh vacuum systems were used in this investigation. An apparatus that is capable of measuring adhesion, load, and friction was mounted in an ultrahigh

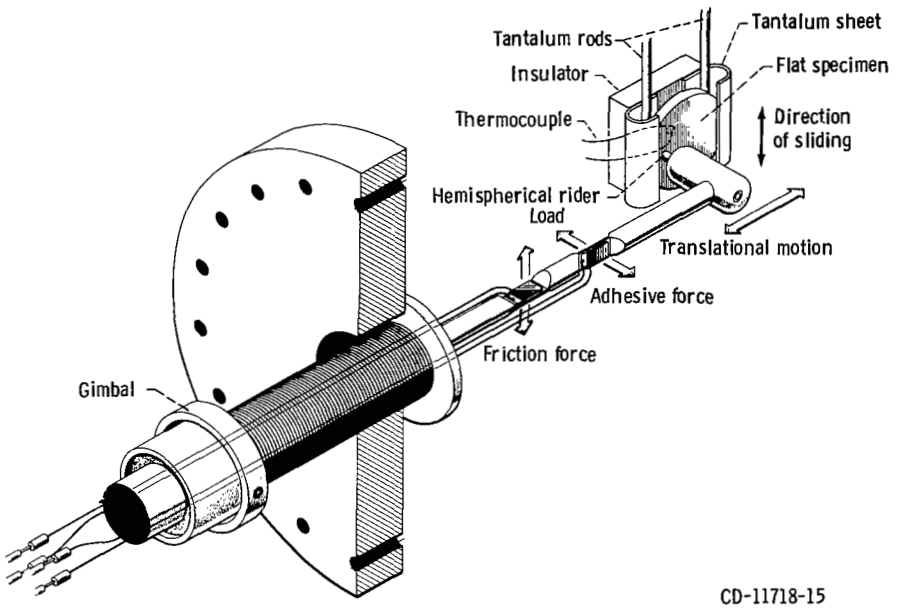

Figure 1. - High-vacuum friction and wear apparatus.

vacuum system (see fig. 1). The vacuum system contained an Auger emission spectrometer (AES). A gimbal mounted beam is projected into vacuum. The beam contains two flats machined normal to each other with strain gages mounted thereon. The iron metal pin is mounted on the end of the beam. The load is applied by moving the beam normal to the flat and is sensed with a strain gage. The vertical sliding motion of the pin along the flat surface is accomplished through a motorized gimbal assembly. Under an applied load, the friction force is measured during vertical translation by the strain gage mounted normal to that used to measure load. This feature was used to examine the coefficient of friction at various loads reported in reference 2.

The second ultrahigh vacuum system contained an X-ray photoelectron spectrometer (XPS) and is shown schematically in figure 2. The figure indicates the major components, including the electron energy analyzer, the X-ray source, and the ion gun used for ion sputter-etching. The X-ray source, contains a magnesium anode. The specimens are mounted on the end of the specimen introduction probe at an angle of 60° with respect to the analyzer axis. The X-ray source is located at an angle of 79° to the analyzer axis. The ion gun is located at an angle of 72° to the analyzer axis.

Experimental Procedure

Specimen Preparation and Heating

In order to heat silicon carbide specimens by resistance heating, a thin-film tantalum coating was applied to the back surfaces of the silicon carbide crystals in a commercial radiofrequency diode sputtering apparatus. After coating, the sliding surfaces of silicon carbide specimens were polished and cleaned, first, with a diamond powder (3 μm diameter) and then the aluminum oxide powder (1 μm diameter). The back surfaces of specimens containing the tantalum films were attached to the tantalum rods or sheets with tantalum supporting sheets (figs. 1 and 2). The tantalum coating surface of the specimen was directly in contact with rods or sheets. The flat and pin surfaces were rinsed with 200-proof ethyl alcohol just before they were placed in the vacuum chamber.

The specimens were placed in the vacuum chamber (figs. 1 and 2), and the system was evacuated and subsequently baked out to obtain a pressure of 10^{-8} pascal (10^{-10} torr). The silicon carbide was heated to about 80° C during baking out. Argon gas was bled back into the vacuum chamber to a pressure of 1.3 pascal, and the pin specimen was argon-ion bombarded for 30 minutes at a −1000-volt direct current potential. The vacuum chamber was then reevacuated.

Surface treatments were conducted in-situ on the silicon carbide flat specimens in both vacuum chambers. The surface treatments with the crystal in the as-received state examined include a heating to a maximum temperature of 1500° C at a pressure of 10^{-8} pascal and subsequent cooling to room temperature after bake-out of the vacuum chamber. Surface of silicon carbide was resistance heated at various temperatures starting at 250° C. The specimen was heated for periods of 1 hour at a pressure of 10^{-8} pascal and cooled to room temperature. Either AES or XPS spectra of the specimen was obtained before and after heating. Specimens were also heated to 400°, 500°, 700°, and 800° C, respectively. All of AES and XPS analyses after coolings were conducted in the same manner as those at 250° C with heating times also

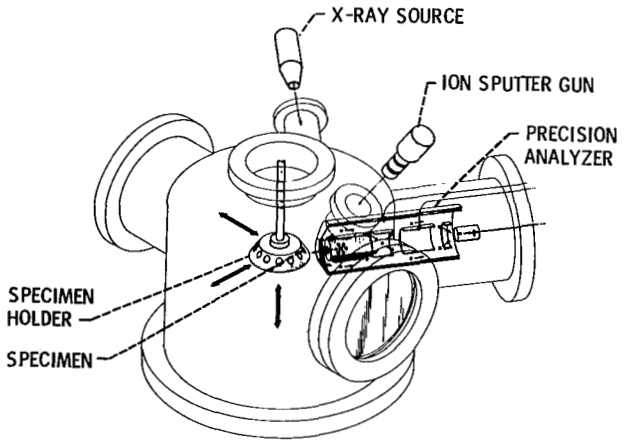

(a) SPECTROMETER.

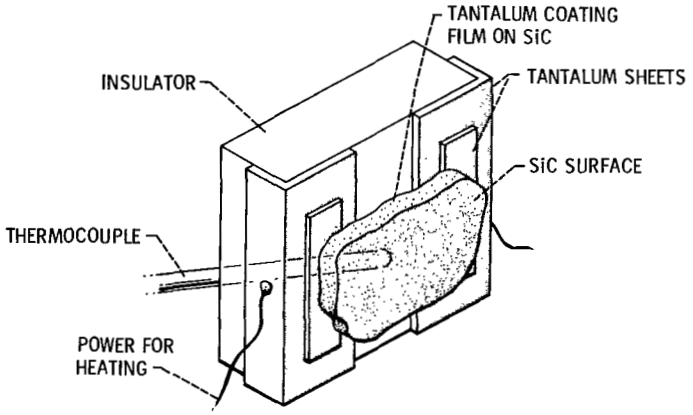

(b) SPECIMEN HOLDER.

Figure 2. - Schematic representations of the X-ray photoelectron spectrometer and silicon carbide specimen.

of 1 hour at each temperature in a vacuum of 10^{-8} pascal.

The power for resistance heating of silicon carbide specimen is supplied through the tantalum rods or sheets and the coated tantalum film by a precisely regulated dc output, adjustable over a wide range. The temperature of the silicon carbide surface was measured with a conventional thermocouple in direct contact with the surface of the silicon carbide specimen. For a depth profiling analysis argon gas was bled back into the vacuum chamber to a pressure of approximately 7×10^{-4} pascal, and the flat specimen was argon-ion bombarded.

Chemical Analyses of Surface

Recent articles describe both AES and XPS (refs. 3 and 4). The techniques provide analyses of the first few atom layers of the surface of the specimens. The analysis depth with AES is of the order of 1 nanometer, and elemental concentrations as low as 0.1 percent of a monolayer can be detected and identified. The analysis depth with XPS is of the order of 2 nanometers, and the ultimate sensitivity is sufficient to allow fractions of a monolayer to be detected and identified.

Many applications of AES and XPS have been made to fundamental tribology studies (refs. 5 to 7). Both qualitative and quantitative information can be obtained with AES and XPS for all elements in the periodic table above helium, and adjacent elements are clearly distinguished. With hydrogen and helium, there are not enough occupied energy levels for detection of these elements. The measurements were conducted in a vacuum systems (10^{-8} Pa)

X-ray Photoelectron Spectroscopy

To obtain reproducible results, a strict standardization of the order and time of recording was used. The instrument was regularly calibrated. The analyzer work function was determined assuming the binding energy for the gold $4f_{7/2}$ peak to be 83.8 electron volts (used as the reference line). All survey spectra, scans of 1050 or 1100 electron volts, were taken at a pass energy of 50 or 100 electron volts, providing an instrumentation resolution of 1 electron volt at room temperature. The Mg K_α X-ray were used with an X-ray source power of 400 watts (10 kV, 40 mA). The narrow scans of the C_{1s}, Si_{2p}, and O_{1s} are just wide enough to encompass the peaks of interest and were obtained with a pass energy of 25 electron volts at room temperature.

Resolution of the spectral peak for silicon is 1.5 electron volts full width at half maximum. The energy resolution is 2 percent of the pass energy, that is, 0.5 electron volts. The peak maxima can be located to ± 0.1 electron volts. The reproducibility of peak height was good, and the probable error in the peak heights ranged from ± 2 to ± 8 percent. Peak ratios were generally good to ± 10 percent or less. There was no evidence for charging of the silicon carbide surface during XPS analysis.

Depth Profiling

The specimen was depth profiled in order to obtain its elemental composition and structure with depth. Before the ion sputtering the chamber pressure was 3×10^{-8} pascal (2×10^{-10} torr) or lower, and the ion gun was outgassed for 2 minutes at a degas emission current of 20 milliamperes. The sublimation pump was then flashed on for about 2 minutes at 48 amperes. The ion pumps are then shut off. The inert gas, argon, was bled in through the leak value to the desired pressure of 7×10^{-4} pascal (5×10^{-6} torr). The ion sputtering was performed with a beam energy equal to 3000 electron volts at 20 milliamperes of beam current with the argon pressure maintained at 7×10^{-4} pascal for the desired sputtering time. The ion beam was continuously rastered over the specimen surface. After sputtering, the system was reevacuated to a pressure of 3×10^{-8} pascal, or lower, and then the surface was examined with the XPS.

The depth, in terms of a sputtering time, was obtained by average measurements of 10 surface-profile records. The profilometer records made on the silicon carbide surface included the underlying area in the same region in which a series of ion sputtering had been done.

Friction Experiments

In-situ single-pass sliding friction experiments were conducted with the surface-treated silicon carbide specimens over a range from room temperature to 1200° C. Loads of 0.2 newton were applied to the pin-flat contact by deflecting the beam of figure 1. To obtain consistent experimental conditions, the time in contact before sliding was 30 seconds. Both the load and friction force were continuously monitored during a friction experiment. Sliding velocity was 3×10^{-3} meter per minute with a total sliding distance of 2 to 3 millimeters at a sliding time of 40 to 60 seconds. All friction experiments were conducted in vacuum with the system evacuated to a pressure 10^{-8} pascal.

Results and Discussion

Depth Profile of Graphitized Surface of Silicon Carbide

The AES spectra of a heated surface of silicon carbide revealed a carbide-type carbon peak in the heating temperature range of from 250° to 800° C. The carbide-type carbon AES peaks are characterized by three peaks labelled A_0 to A_2 in figure 3.

The carbide-type carbon peak changed to the graphite-type at 900° to 1000° C, while the silicon peak decreased in intensity. The decrease of silicon peak intensity is due to preferential evaporation of silicon from the silicon carbide surface (refs. 8 and 9). The spectra of the surface

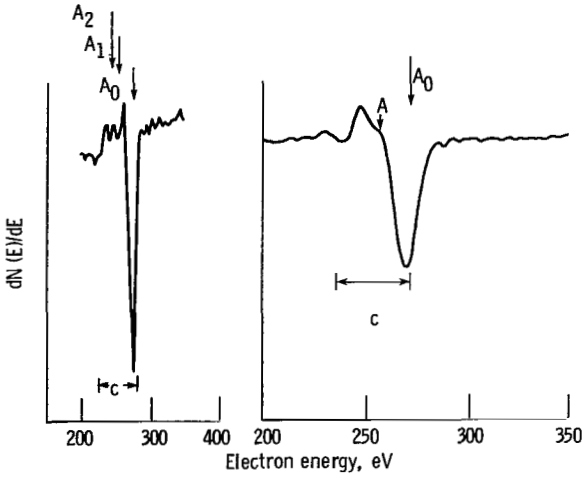

(a) Carbide type. (b) Graphite type.

Figure 3. - Auger peaks of carbon on a silicon carbide {0001} surface.

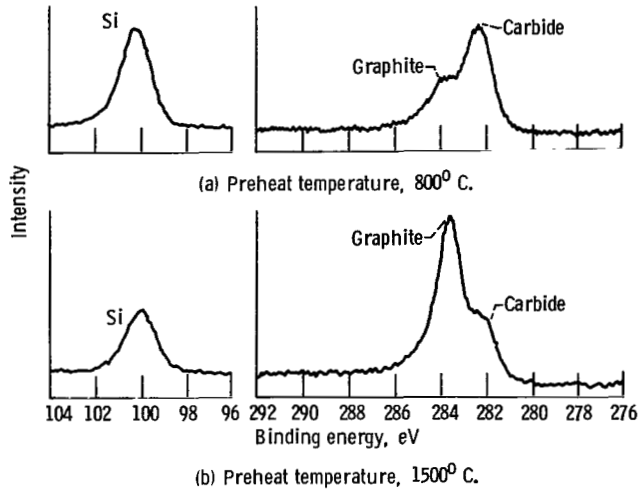

Figure 4. - Representative Si2p and C1s XPS peaks on the silicon carbide {000} surface preheated at temperatures of 800° and 1500° C.

heated in the temperature range 1000° to 1500° C clearly revealed two characteristics: (1) a graphite-type carbon peak increase and (2) the decrease of silicon peak with increasing temperature. The mechanism for graphite formation is that two successive carbon layers on the surface of silicon carbide, after the evaporation of silicon, collapse into one layer of carbon hexagons with the unit mesh parallel to that of silicon carbide (refs. 8 to 9). Figure 3(b) shows the typical graphite-type carbon peak. The graphite form is characterized by a step (labelled A in the figure).

XPS spectra of C_{1s} and Si_{2p} obtained from the single-crystal silicon carbide surface are presented in figure 4. The vertical height, peak to base line, of the Si_{2p} peak in the spectra was highest at 800° C. Above 800° C, the Si_{2p} decreased gradually with increasing temperature.

Photoelectron lines for C_{1s} of the silicon carbide are split asymmetrically into doublet peaks. The results represent a significant temperature influence on the silicon carbide surface as well as those of AES analysis.

The doublet peaks are due to distinguishable forms of carbon, that is, the graphite and carbide. A large carbide-peak is clearly observed at 800° C, while a very large graphite peak is clearly observed above 1200° C (ref. 10).

AES analysis of silicon carbide preheated above 1200° C (as typically shown in fig. 3) indicated that the silicon AES peak had almost disappeared and was nearly undetectable by AES and that the carbon peak was only of the graphite form (refs. 1 and 2). But XPS analysis clearly indicated the evidence for silicon and carbide as well as graphite being present on the silicon carbide surface preheated above 1200° C.

The graphitization behavior in the outermost surficial layer is believed to be as follows: The analysis depth with AES is of the order of 1 nanometer, and an elemental concentration as low as 0.1 percent of a monolayer can be detected and identified. The analysis depth with XPS is of the order of 2 nanometers, and the ultimate sensitivity is sufficient to allow fractions of a monolayer to be

detected and identified. Therefore, the outermost surficial layer, which consists of mostly graphite and very little silicon, on the silicon carbide surface, is anticipated to be of the order of 2 nanometers.

Consider the outermost surficial layer that is graphitized. The methods of determining the outer graphite layer are to study either the attenuation by the graphite layer of a photoelectron originating in the bulk material of silicon carbide or the variation in intensity of photoelectrons emitted by the layer itself as a function of thickness. The photoelectron flux penetrating a layer thickness d is simply

$$I_d = I_o \exp(-d/\lambda) \tag{1}$$

where I_d is the flux emerging at the surface, that is, the XPS peak intensity from the layer of a thickness d, I_o is the flux emitted by the clean silicon carbide, and is variously referred to as the inelastic mean free path, the mean escape depth or the attenuation length of an electron with the electron energy of the material being examined (refs. 11 and 12). On the other hand, the intensity of a photoelectron signal from the layer is

$$I_d = I_o[1 - \exp(-d/\lambda)] \tag{2}$$

In either case, the mean escape depth relates λ to the material of the layer and to electrons of a given kinetic energy. The potential value varies the angle of electron emission, or takeoff angle θ in XPS experiments. The generalized theoretical predictions for intensity changes with θ for the bulk silicon carbide. The graphite overlayer system is given by

$$I_d = I_o(1 - e^{-d/\lambda \sin\theta}) \tag{3}$$

Table I shows inelastic mean free paths of various elements and the estimated thickness of the graphite layer formed on the silicon carbide surface. The data values in table I have been estimated with the equations above using the values of λ for silicon, carbon, and graphite of the references 12 and 14. The above-mentioned angular

TABLE I. - VALUES FOR THE THICKNESS OF THE GRAPHITE LAYER ON THE SILICON CARBIDE SURFACE PREHEATED TO 1500° C

Element and photoelectron (Mg kα)	Electron inelastic mean free path, λ, nm	Thickness of layer, d, nm
Si_{2p}	[a]4.7	2.0
	[a,b]3.9	1.7
C_{1s}	[b]4.4	1.8
Graphite C_{1s}	[a]2.1	1.5
	[a]3.1	2.3
	[a]3.4	2.4

[a]Ref. 14.
[b]Ref. 15.

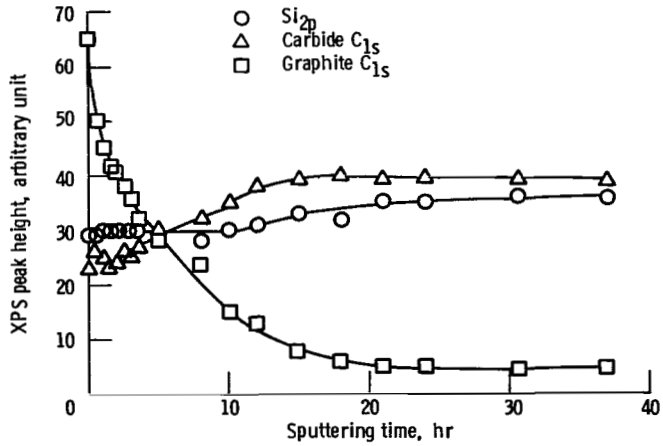

Figure 5. - Elemental depth profile of silicon carbide {0001} surface preheated at temperature 1500° C for 1 hour.

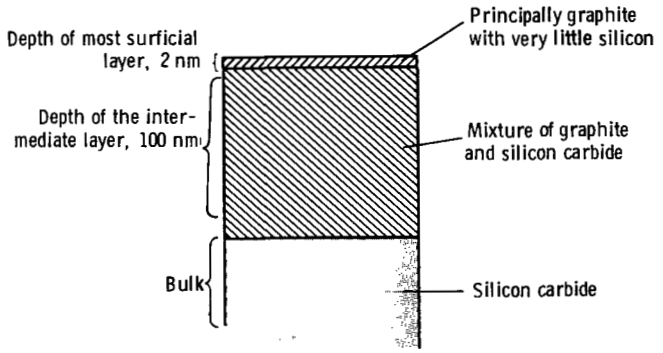

Figure 6. - Surface condition of silicon carbide after heating at temperatures above 1200° C.

variation took the estimation into account. The thickness of the outermost surficial graphite layer on the silicon carbide heated to 1500° C is therefore 1.5 to 2.4 nanometers. This thickness is consistent with the position of Bommel, et al. (ref. 9), that is, the collapse of the carbon of three successive silicon carbide layers is the most probable mechanism for the initial stages of the graphitization of silicon carbide basal planes.

A typically complete elemental depth profile for the silicon carbide surface preheated to 1500° C is shown as a function of sputtering time in figure 5. The graphite peak decreases rapidly in the first 30 minutes of sputtering; thereafter it gradually decreases to 18 hours. The depth after 37 hours of sputtering was 200 to 400 nanometer the area analyzed by XPS. This depth was measured by the profilometer. If the depths sputtered at corresponding times are approximately the same (because the materials were almost same), the depth at the sputtering time of 18 hours is 100 to 200 nanometers. The depth of the mixture of graphite and silicon carbide is of the order of 100 nanometers, which is schematically shown in figure 6.

Ellipsometric measurements have been conducted with two different {0001} faces of the first atomic layer of the silicon carbide surface, one which consisted of silicon

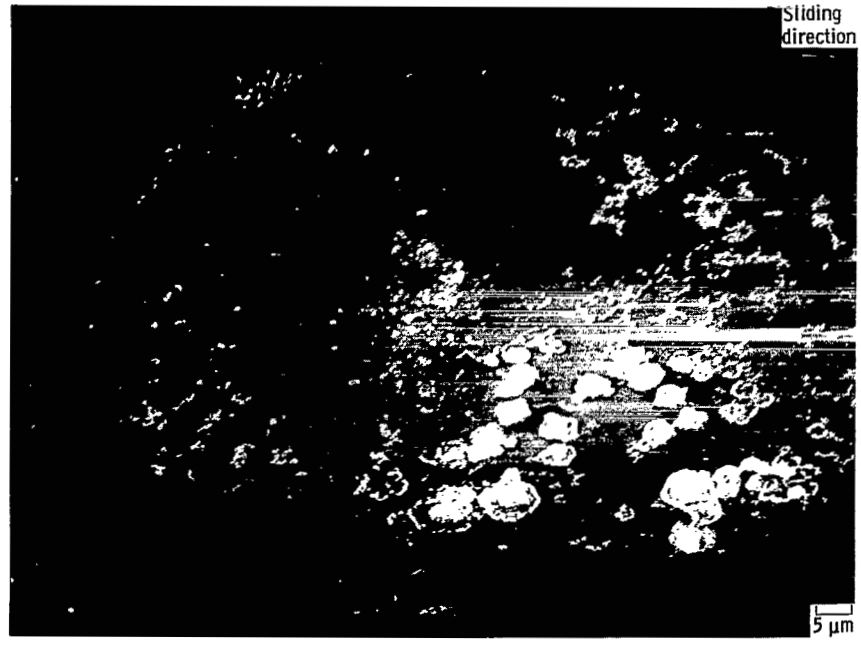

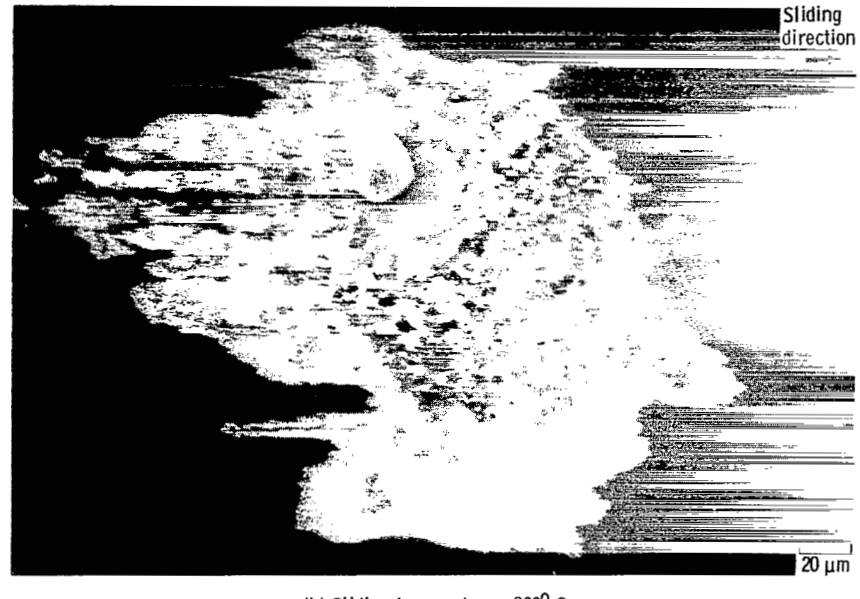

(b) Sliding temperature, 800° C.

Figure 7. - Iron transferred to single-crystal silicon carbide at commencement of sliding as a resul of a single pass of rider. Silicon carbide {0001} surface; sliding direction <10$\bar{1}$0>; sliding velocity, 2 mm/min.; load, 0.2 N; vacuum pressure, 10^{-8} Pa.

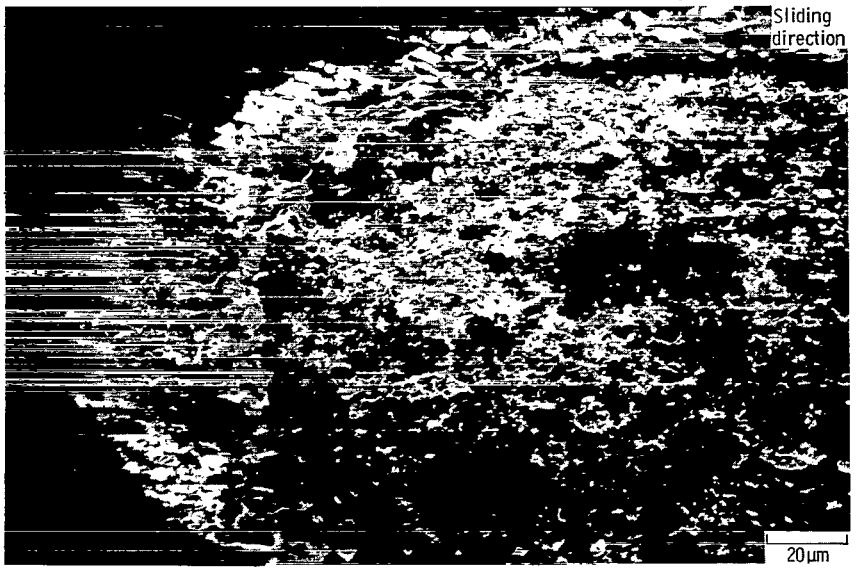

(c) Sliding temperature, 1200° C.

Figure 7. - Concluded.

atoms {0001} and the other which consisted of carbon atoms {0001} at temperatures above 1200° C (ref. 15). In 1 hour of heating at 1300° C, the layer, which consists of carbon (graphite), on the C-face grows to about 100 nanometers, whereas the layer on the Si-face did not grow thicker than 10 nanometers even with longer heating.

The first atomic layer of the silicon carbide {0001} surfaces used in this investigation is a mixture of silicon-face and carbon-face because the surfaces were mechanically polished. Again, the apparent thickness of the graphite layer, which consists of graphite produced by heating above 1200° C for 1 hour as measured by the profilometer is approximately 100 nanometers, and it is equivalent to the depth of the graphite layer on the silicon carbide measured in reference 15, which consisted of a carbon-face of silicon carbide. The results of XPS analyses and depth profiling conducted in this investigation with silicon carbide {0001} surfaces heated to 1500° C were used to summarize the surface condition of silicon carbide (fig. 6).

Metal Transfer

Inspection of the single-crystal silicon carbide surface after sliding contact with iron revealed transfer of iron to silicon carbide. Figure 7 shows scanning electron micrographs at the beginning of the wear tracks generated by a single pass of the iron on the surface at sliding temperatures of room, 800° and 1200° C. As may be seen, sliding at 800° C produces more metal transfer than does sliding at room temperature. In general, a very thin transfer film and very small particles are seen in the contact area. The higher the sliding temperature, the more transfer produced. Above 800° C (fig. 7(c)), however, there was very little evidence for a smooth and continuous transfer film on the wear track; rather transfer was rough, and discontinuous.

The appearance of iron transfer may relate to the graphite layer (on the order of to 2 nm) on the silicon carbide surface.

Fracture Wear

The sliding of iron on a silicon carbide surface at elevated temperatures results in the formation of cracks and fracture pits in the silicon carbide surface. The wear due to fracture occurs very locally and in very small areas in the sliding contact region. The development of cracks generally follows stress trajectories and cleavage planes.

Figure 8 presents scanning electron micrographs of the wear track on the silicon carbide surface, where the wear track is generated by a single-pass sliding of the iron rider at 800° C. The wear track has in it microfracture pits and silicon carbide debris. Two kinds of fracture pits are generally observed in the wear track: (1) pit with a spherical particle, and (2) pit with a multiangular-shaped wear debris particles, which have crystallographically oriented sharp edges and which are of a platelet hexagonal shape.

Such multiangular wear debris are generated by surface cracking along $\{10\bar{1}0\}$ or $\{11\bar{2}0\}$ and subsurface cracking along {0001} planes, which are parallel to the sliding interface. Figure 9 presents a scanning electron micro-

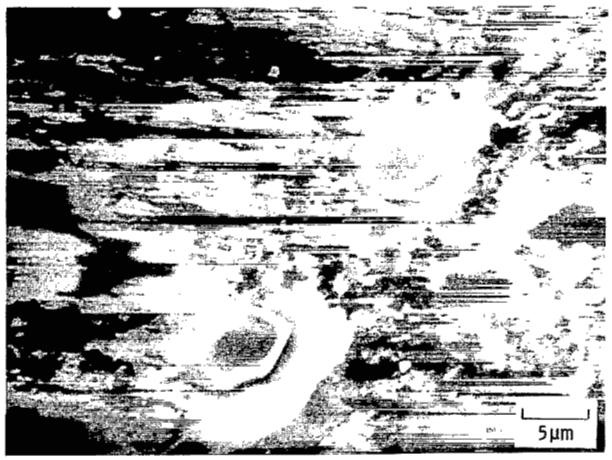

(a) Wear track.

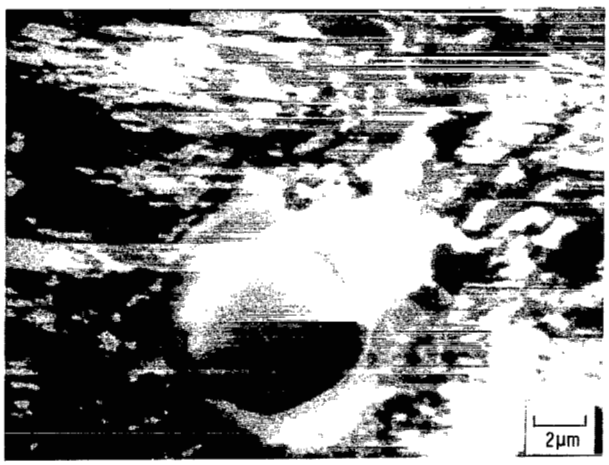

(b) Pit with a spherical wear debris.

(c) Pit with a hexagonal shaped wear debris.

Figure 8. - Scanning electron micrographs of wear track on silicon carbide {0001} surface. Single pass sliding of iron rider; sliding velocity, 3 mm/min; load, 0.2 N; temperature, 800° C; vacuum pressure, 10^{-8} Pa.

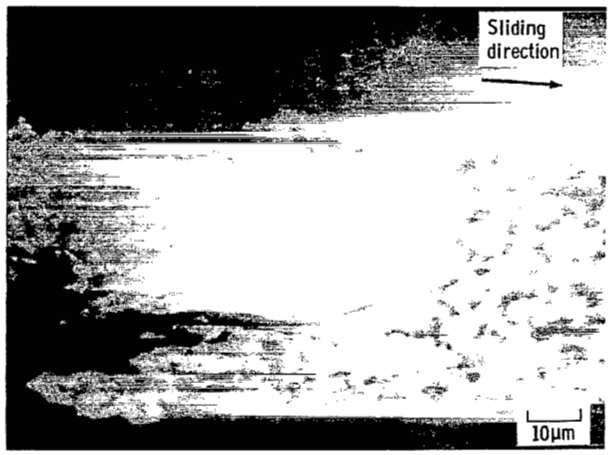

Figure 9. - Cracking of single-crystal silicon carbide {0001} surface in contact with iron rider as a result of single pass at 800° C in vacuum (10^{-8} Pa). Scanning electron micrograph; sliding direction, 10$\bar{1}$0; sliding velocity, 3 mm/min; load, 0.2 N; temperature, 800° C; vacuum pressure, 10^{-8} Pa.

graph of wear track of silicon carbide generated by sliding on iron at 800° C. Fracture of the silicon carbide surface occurred as a result of cleavage. The smooth surface of the fracture pit is due to subsurface cleavage along {0001} planes. Very thin silicon carbide wear debris platelets have already been ejected from the wear track. The crystallographically oriented cracking around the fracture pits occurred in the {10$\bar{1}$0} and {11$\bar{2}$0} planes. Thus, the fracture of the silicon carbide {0001} surface and the generation of multiangular wear debris platelet are related to the surface and subsurface cleavage along {10$\bar{1}$0}, {11$\bar{2}$0}, and {0001} planes. This fracture mechanism is consistent with earlier studies of silicon carbide in sliding contact with metals and itself at room temperature (refs. 16 and 17).

It is understandable that the fracturing in the single crystal of silicon carbide is characterized by crystallographic orientation. However, the appearance of fracture pits with a spherical shape is an interesting observation.

Figure 10 presents scanning electron micrographs of various fracture pits with spherical wear debris in the very local area of wear tracks. These results reveal that a nearly spherical particle can exist in the fracture pit. In other words a spherical fracture can occur in the single-crystal silicon carbide under the sliding surface with sliding friction. Such fracture pits with the spherical particles were observed in the friction experiments involving the high friction (coefficient of friction of about 0.8).

It was found in reference 16 that spherical wear debris of silicon carbide are observed as a result of sliding friction experiments with iron binary alloys. In these cases, the friction was also high. The coefficient of friction was generally higher than unity. The spherical particles have been observed only at the condition of high friction at sliding temperatures of 400° to 800° C. The

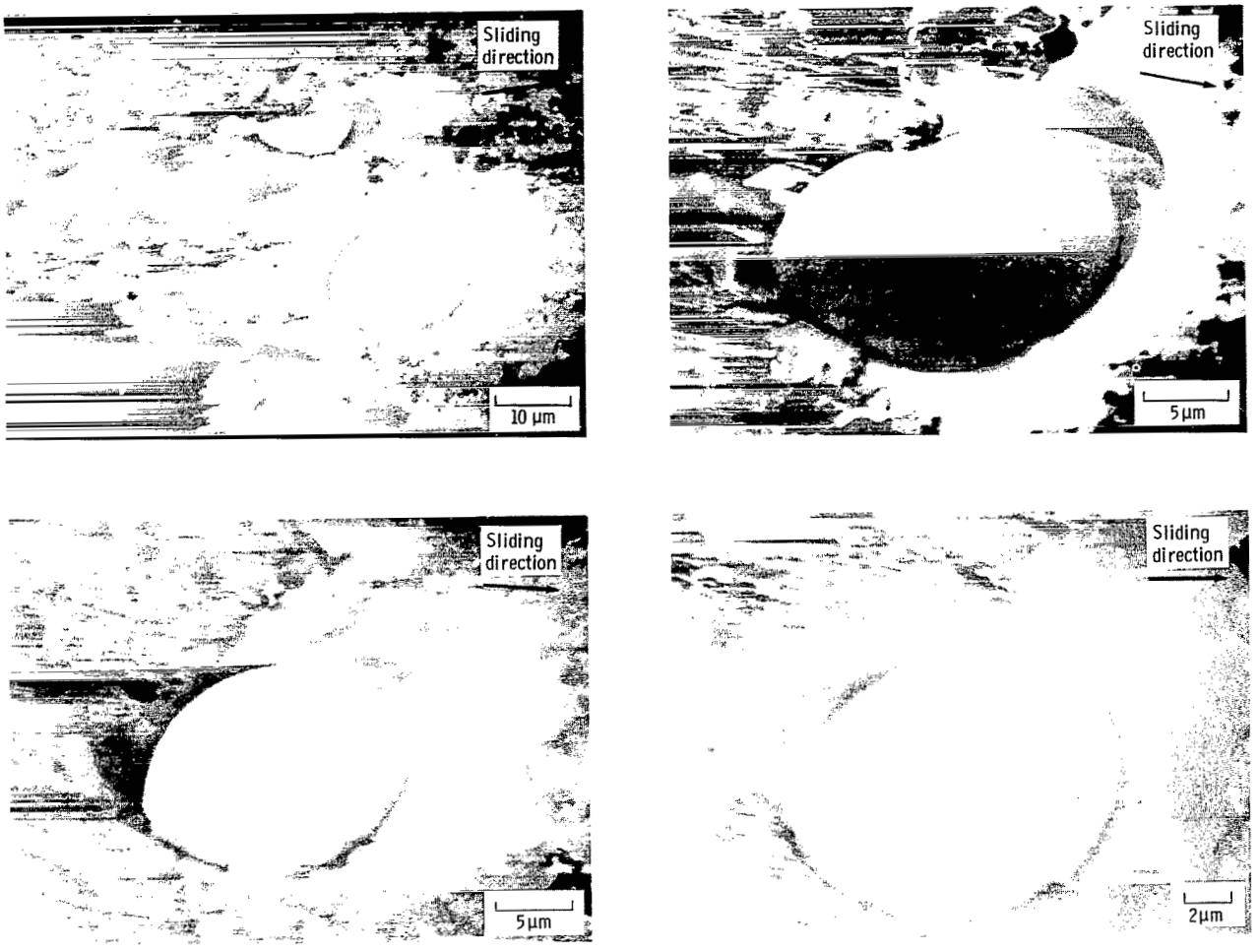

Figure 10. - Fracture pits with sperical wear debris obtained in different experiments but under the same conditions. Single pass sliding of iron rider; sliding velocity, 3 mm/min; load, 0.2 N; temperature, 800° C; vacuum pressure, 10^{-8} Pa.

generation of the spherical particles may be related to the high friction.

A mechanism for the generation of fracture pit with a spherical wear debris seems to be very similar to that of spherical wear particles described in reference 16.

Three possible mechanisms for the generation and formation of the spherical wear debris particle are considered herein: (1) a spherical-shaped crack along the circular stress trajectories, (2) an attrition of wear particles (ref. 17), and (3) a rolling into a ball-shaped particle due to surface energy. The second mechanism is not applied to the fracture pit with the spherical wear debris because the spherical wear debris was not ejected from the silicon carbide surface. The third mechanism does not apply to the fracture pit, because silicon carbide is a very brittle material. The only possible mechanism is therefore the first one, that is, the spherical-shaped cracking.

Consider the primary fracture mechanism of silicon carbide in the sliding process reported herein: the wear debris of the iron and silicon carbide, which transferred to the counter surfaces or were dislodged, and fracture pits in the wear track can produce local stress concentration at the interface (shown schematically in fig. 11). There are small silicon carbide and iron wear particles and/or fracture pits at the interface.

The stress concentration at the sharp edges of wear debris or fracture pits may produce a small zone of inelastic deformation in silicon carbide about the sharp edge. Cracks will subsequently be initiated in the two possible favored geometries (see figs. 12 and 13 (refs. 18 and 19)). Figure 12 indicates that (1) the sharp point produces a plastic deformation region, (2) a deformation-induced flow or crack produced in the sliding develops into a crack or growth of a crack subsurface from the inelastic deformation zone, (3) on application of sliding friction force the crack closes or expands and secondary cracks begin to develop, and (4) the cracks grow steadily below the subsurface. Such fracture may produce the multiangular silicon carbide wear debris during sliding, as already mentioned.

Figure 13 indicates another possible cracking

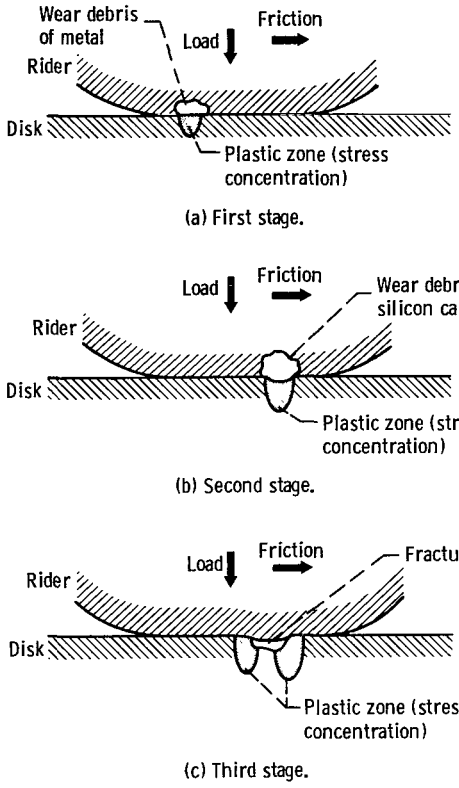

Figure 11. - Sources of stress concentration under loading and sliding conditions.

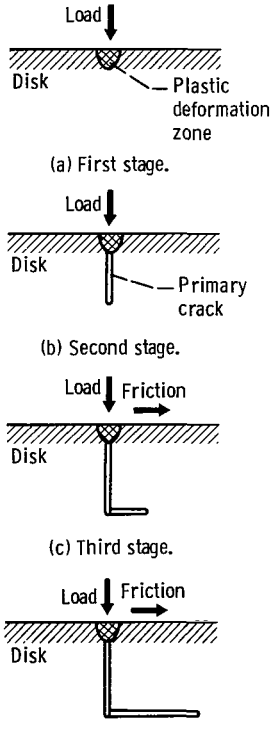

Figure 12. - Crack formation under inelastic and deformation zone.

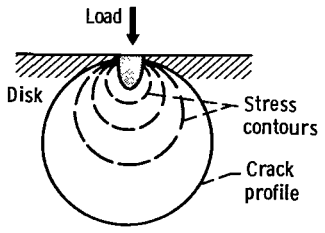

Figure 13. - Spherical crack formation under inelastic deformation zone (ref. 15).

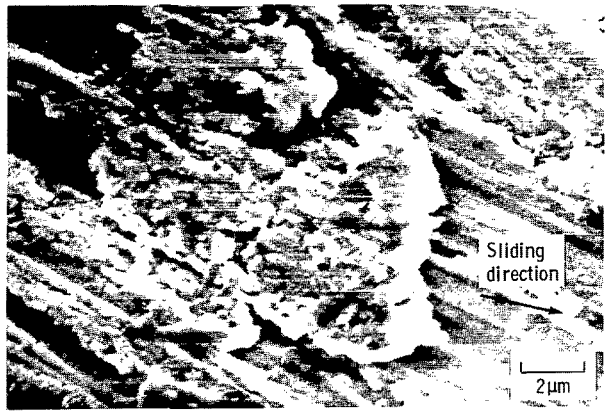

(a) Wear scar.

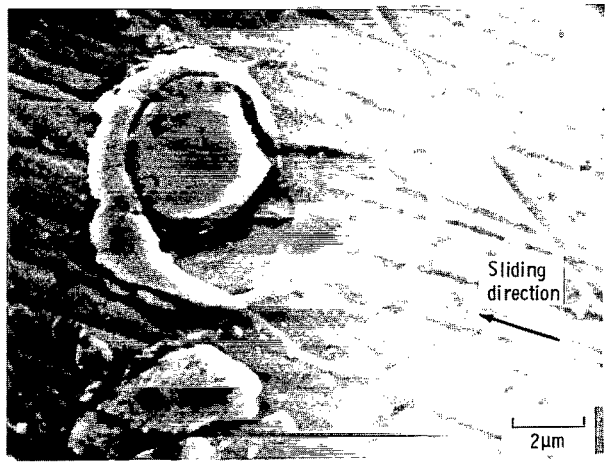

(b) Silicon carbide wear debris on iron wear scar.

Figure 14. - Silicon carbide wear debris on iron rider wear scar as a result of single pass sliding. Scanning electron micrographs; sliding velocity, 3 mm/min; load, 0.2 N; temperature, 800° C; vacuum pressure, 10^{-8} Pa.

mechanism, that is, sudden development of a spherical-shaped crack along the circular stress trajectories. It is known that this "penny-shaped" crack is produced in amorphous materials such as soda-lime glass under Vickers indentations (ref. 19). The influence of crystallinity, however, is imposed on the crack geometries of anisotropic materials such as silicon carbide, and

accordingly the present crack geometry is observed. Therefore, the spherical-shaped cracks may not be a circle in silicon carbide. But the possibility of a fracture such as the one shown in figure 13, that is, a nearly circular or spherical fracture, would still exist in a single crystal because it is possible that the cracks would grow and pick up in atomistic terms by the sequential rupture of cohesive bonds along the circular stress trajectories shown in figure 13. This fracture mechanism may explain the possibility of generating fracture pit with a spherical particle.

Lately, sliding of iron on a silicon carbide surface results in both the transfer of iron to silicon carbide, which was described earlier, and very occasionally a transfer of silicon carbide wear debris to the iron rider. Figure 14 presents scanning electron micrographs of wear scars on a iron rider after it slid on a silicon carbide surface at 800° C in vacuum. The wear scars reveal a large number of plastically deformed grooves. Figure 14 indicates that wear debris of silicon carbide produced during sliding transferred to the iron rider. This fact is consistent with the earlier works (refs. 16 and 17).

Summary of Results

AES and XPS analyses and sliding friction and wear experiments with single-crystal silicon carbide {0001} surface heated to 1500° C revealed the following:

1. The outer most surficial layer of silicon carbide consists of mostly graphite and very little silicon at temperatures above 1200° C. This graphite layer is 1.5 to 2.4 nanometers. There is an intermediate layer, consisting of a mixture of graphite, carbide, and silicon, which is about 100 nanometers thick.

2. The higher the sliding temperature, to 800° C, the greater the metal transfer in a smooth, thin, and continuous film. Above 800° C, the transfer is rough and discontinuous.

3. Two kinds of fracture pits are observed on the silicon carbide surface: (1) a pit with a spherical particle and (2) a multiangular shaped pit. The former may be produced by a mechanism of a spherical-shaped fracture along the circular stress trajectories under the local inelastic deformation zone. The latter, multiangular fracture pit is believed to be produced by primary and secondary cracking along the cleavage planes {0001}, $\{10\bar{1}0\}$, $\{11\bar{2}0\}$.

4. The spherical fracture pits have been generally observed only at the condition of high friction at sliding temperatures of 400° to 800° C.

Lewis Research Center
National Aeronautics and Space Administration
Cleveland, Ohio, May 1, 1981

References

1. Miyoshi, K.; and Buckley, Donald H.: Changes in Surface Chemistry of Silicon Carbide (0001) Surface with Temperature and Their Effect on Friction. NASA TP-1756 (1980).
2. Miyoshi, K.; and Buckley, Donald H.: Surface Chemistry and Friction Behavior of the Silicon Carbide (0001) Surface at Temperatures to 1500° C. NASA TP-1813 (1981).
3. Swingle, Robert S., II and Riggs, W. M.: ESCA. CRC Crit. Rev. Anal. Chem., vol. 5, no. 3, 1975, pp. 267-321.
4. Kane, P. F.; and Larrabee, G. B.; eds.: Characterization of Solid Surfaces. Plenum Press, 1974.
5. Buckley, Donald H.: The Use of Analytical Surface Tools in the Fundamental Study of Wear. Wear, vol. 46, 1978, pp. 19-53.
6. Wheeler, Donald R.: X-ray Photoelectron Spectroscopic Study of Surface Chemistry of Dibenzyl Disulfide on Steel under Mild and Severe Wear Conditions. Wear, vol. 47, 1978, pp. 243-254.
7. Ferrante, John: Practical Applications of Surface Analytic Tools in Tribology. NASA TM-81484, 1980.
8. Badami, D. V.: X-ray Studies of Graphite Formed by Decomposing Silicon Carbide. Carbon, vol. 3, no. 1, 1965, p. 53-57.
9. Van Bommel, A. J.; Crombeen, J. E. and Van Tooren, A.: LEED and Auger Electron Observations of the SiC (0001) Surface. Surf. Sci., vol. 48, 1975, pp. 463-472.
10. Wagner, C. D.; et al.; eds.: Handbook of X-ray Photoelectron Spectroscopy. Perkin-Elmer Corp., 6509 Flying Cloud Drive, Eden Praire, Minnesota.
11. Orchard, A. F.: Basic Principles of Photoelectron Spectroscopy. Handbook of X-ray and Ultraviolet Photoelectron Spectroscopy. D. Briggs, ed. Heyden, London, 1977, pp. 1-77.
12. Briggs, D.: X-ray Photoelectron Spectroscopy as an Analytical Technique. Handbook of X-ray and Ultraviolet Photoelectron Spectroscopy D. Briggs, ed. Heyden, London, 1977, pp. 153-181.
13. Evans, Stephen; Pritchard, Robin G.; and Thomas, John M.: Escape Depths of X-ray (Mg-α)-induced photoelectrons and relative photoionization cross sections for the 3p subshell of the elements of the first long period. J. Phys. C., vol. 10, no. 13, July 1977, pp. 2483-2498.
14. Cadman, Philip; et al.: Determination of Relative Electron Inelastic Mean Free Paths (Escape Depths) and Photoionization Cross-Sections by X-ray Photoelectron Spectroscopy. J. Chem. Soc., Faraday Trans. II, vol. 71, no. 10, 1975, pp. 1777-1784.
15. Meyer, F.; Loyen, G. J.: Ellipsometry Applied to Surface Problem—Optical Layer Thickness Measurement. Acta Electron., vol. 18, Jan. 1975, pp. 33-38.
16. Miyoshi, K.; and Buckley D. H.: Friction and Fracture of Single-Crystal Silicon Carbide in Contact with Itself and Titanium. ASLE Trans., vol. 22, no. 2, Apr. 1979, pp. 146-153.
17. Miyoshi, K.; and Buckley, D. H.: The Generation and Morphology of Single-Crystal Silicon Carbide Wear Particles under Adhesive Conditions. Wear vol. 67, no. 3, 1981, pp. 303-319.
18. Mikosza, A. G.; and Lawn, B. R.: Section-and-Etch Study of Hertzian Fracture echanics. J. Appl. Phys., vol. 42, no. 13, Dec. 1971, pp. 5540-5545.
19. Lawn, B. R.; and Swain, M. W.: Microfracture Beneath Point Indentations in Brittle Solids. J. Mater. Sci., vol. 10, no. 1, Jan. 1975, pp. 113-122.

1. Report No. NASA TP-1947	2. Government Accession No.	3. Recipient's Catalog No.
4. Title and Subtitle SURFACE CHEMISTRY AND WEAR BEHAVIOR OF SINGLE-CRYSTAL SILICON CARBIDE SLIDING AGAINST IRON AT TEMPERATURES TO 1500° C IN VACUUM		5. Report Date February 1982 6. Performing Organization Code 506-53-22
7. Author(s) Kazuhisa Miyoshi and Donald H. Buckley		8. Performing Organization Report No. E-654 10. Work Unit No.
9. Performing Organization Name and Address National Aeronautics and Space Administration Lewis Research Center Cleveland, Ohio 44135		11. Contract or Grant No.
12. Sponsoring Agency Name and Address National Aeronautics and Space Administration Washington, D.C. 20546		13. Type of Report and Period Covered Technical Paper 14. Sponsoring Agency Code

15. Supplementary Notes

16. Abstract

X-ray photoelectron and Auger electron spectroscopy analyses and morphological studies of wear and metal transfer were conducted with a single-crystal silicon carbide {0001} surface in contact with iron at various temperatures to 1500° C in a vacuum of 10^{-8} pascal. The results indicate that below 800° C, carbide-carbon and silicon are primarily seen on the silicon carbide surface. Above 800° C the graphite increases rapidly with increase in temperature. The outermost surficial layer, which consists mostly of graphite and little silicon at temperatures above 1200° C is about 2 nm thick. A thicker layer, which consists of a mixture of graphite, carbide, and silicon is approximately 100 nm thick. The closer the surface sliding temperature is to 800° C, the more the metal transfer produced. Above 800° C, there was a transfer of rough, discontinuous, and thin iron debris instead of smooth, continuous and thin iron film which was observed to transfer below 800° C. In these studies two kinds of fracture pits were observed on the silicon carbide surface: (1) a pit with a spherical asperity and (2) multiangular shaped pits.

17. Key Words (Suggested by Author(s))	18. Distribution Statement
XPS; Wear; SiC	Unclassified - unlimited STAR Category 27

19. Security Classif. (of this report)	20. Security Classif. (of this page)	21. No. of Pages	22. Price*
Unclassified	Unclassified	12	A02

* For sale by the National Technical Information Service, Springfield, Virginia 22161

NASA-Langley, 1982

National Aeronautics and
Space Administration

Washington, D.C.
20546

Official Business
Penalty for Private Use, $300

SPECIAL FOURTH CLASS MAIL
BOOK

Postage and Fees Paid
National Aeronautics and
Space Administration
NASA-451

U.S.MAIL

4 1 1U,C, 022362 S00903DS
DEPT OF THE AIR FORCE
AF WEAPONS LABORATORY
ATTN: TECHNICAL LIBRARY (SUL)
KIRTLAND AFB NM 87117

NASA

POSTMASTER: If Undeliverable (Section 158
Postal Manual) Do Not Return